A Hybrid Optimization Method to Analyze Metamaterial-Based Electrically Small Antennas

Aycan Erentok and Richard W. Ziolkowski, *Fellow, IEEE*

***Abstract*—A model of an idealized radiating system composed of an electrically small electric dipole antenna enclosed in an electrically small multilayered metamaterial shell system is developed analytically. The far-field radiation characteristics of this system are optimized using a GA-MATLAB based hybrid optimization model. The optimized-analytical model is specifically applied to a spherical glass shell filled with a "cold plasma" epsilon-negative (ENG) medium. These analytical results are confirmed using ANSOFT HFSS and COMSOL Multiphysics simulations; these numerical results include input impedance and overall efficiency values not available with the analytical model. The optimized-analytical model is also used to achieve electrically small nonradiating metamaterial-based multilayered spherical shell designs. The optimized shell properties are exploited to obtain multiband radiating and nonradiating response characteristics. Dispersion properties of the ENG materials are also included in all the analytical models; the bandwidth characteristics of these systems are discussed.**

***Index Terms*—Electrically small antennas, genetic algorithm (GA), metamaterials, optimization methods.**

I. Introduction

ANTENNAS that are electrically small, efficient, and have significant bandwidth would fulfill many of today's emerging wireless technology requirements, especially in the areas of communications and sensor networks [1]–[34]. It is well known that an electrically small electric dipole antenna's complex input impedance has a very small radiation resistance and a very large capacitive reactance making it an inefficient radiator [1]–[19]. Consequently, to obtain a high radiation efficiency, considerable effort must be expended on a matching network that produces an impedance that is conjugately matched to the dipole's impedance. A matching network is incorporated that forces the total reactance to zero by introducing a very large inductive reactance which cancels the very large capacitive reactance of the electrically small electric dipole antenna, and that then matches the resistance of this resonant system to the feed network. In another words, it forces the input resistance of this resonant system to be equal to the source impedance value, e.g., 50 Ω. There have been a wide variety of other approaches to achieve electrically small antennas including clever packing of resonant antenna elements into a small volume using natural geometrical configurations [12]–[15], fractal curve antennas [20]–[23] and space-filling curve antennas [24]–[27]. Very nonintuitive structures generated with optimization approaches have also been considered successfully [28]. Recently, a different paradigm for achieving an efficient electrically small antenna (EESA) that has interesting bandwidth characteristics was reported [35]. Metamaterial-based antenna systems can be designed to integrate simply an electrically small dipole antenna with the appropriate single negative (SNG) spherical shell system (electric dipole-epsilon negative (ENG) shell system, magnetic dipole-mu negative (MNG) shell system) [35]–[38] or the corresponding double negative (DNG) spherical shell system [29] to achieve simultaneously a large overall efficiency and a large fractional bandwidth for hypothetical homogenous dispersionless metamaterial media.

It has already been shown that a single suitable metamaterial layer is sufficient to provide the required impedance matching which would enable an electrically small antenna to radiate efficiently into the far-field region [35]. This research work generalizes the electrically small dipole-single metamaterial spherical shell system to an electrically small dipole-multilayered metamaterial spherical shell system. An analytical model for an infinitesimal electric dipole antenna-multilayered metamaterial-based spherical shell system is developed and is combined with a hybrid optimization method to maximize the far-field performance. The analytical model allows a complete understanding of both the near- and far-field behavior of this antenna system. The proposed optimization approach is a combination of the genetic algorithm (GA) and the MATLAB optimization toolbox to achieve a simple but effective and user friendly optimization model. Section II describes the GA and MATLAB optimization details and provides extensive performance comparisons with previously published results. Section III discusses a specific application of the developed analytical model to an electrically small electric dipole antenna in the presence of a spherical glass shell filled with a "cold plasma" ENG medium. A finite numerical model of the corresponding coax-fed monopole within the same multilayered (glass-ENG-glass) system was also simulated using ANSOFT's High Frequency Structure Simulator (HFSS) and COMSOL's Multiphysics package. The numerical models are used to confirm the analytical model's results and to obtain an accurate calculation of the input impedance and the associated overall efficiency. It will be demonstrated that a properly designed electrically small coax-fed monopole-(glass-ENG-glass) shell system will produce a resonant configuration whose total reactance is zero and whose radiated power is a maximum and that the resistance of this resonant configuration can

Manuscript received March 22, 2006; revised September 14, 2006. This work was supported in part by DARPA under Contract HR0011-05-C-0068.

The authors are with the Department of Electrical and Computer Engineering, The University of Arizona, Tucson, AZ 85721-0104 USA (e-mail: erentoka@ece.arizona.edu; ziolkowski@ece.arizona.edu).

Color versions of one or more of the figures in this paper are available online at http://ieeexplore.ieee.org.

Digital Object Identifier 10.1109/TAP.2007.891553

be readily matched to the source impedance to achieve a high overall efficiency. The impact of dispersion on the bandwidth and quality factor of this resonant system is also discussed. In Section IV the analytical model is used to demonstrate that a multilayered ENG spherical shell system can be designed to achieve both efficient and electrically small multiband radiating, as well as nonradiating, systems. Both lossless and lossy dispersive media effects are considered. It is further shown that the number of radiating or nonradiating frequencies depends on the number of shell layers and the values of their relative permittivities. It is also discussed how the multilayered metamaterial spherical shell systems can be used to reduce the mutual coupling in an electrically small dense array of radiators. A summary of the various optimized metamaterial-based electrically small antenna systems considered in this paper is given in Section V.

We note that an ENG shell may be realized artificially with metamaterials or naturally with plasmas. In contrast to previous considerations of the basic dipole-shell configuration for both source and scattering applications [39]–[43], the present work emphasizes the multilayered resonant configurations that exist even when the system is electrically small. Negative permittivity metamaterial element designs to achieve the requisite properties discussed below are in progress and are beyond the scope of this presentation.

As a matter of definitions to be used throughout this paper, an $\exp(+j\omega t)$ time dependence is assumed throughout. In agreement with the definition given by Best in [13], an electrically small antenna in free space is defined by the constraint that $kr_e \leq 1.0$ ($kr_e \leq 0.5$), where r_e is the radius of the smallest sphere (hemisphere) enclosing the entire system and $k = 2\pi/\lambda$ is the wave vector corresponding to the free space wavelength $\lambda = c/f$, f being the frequency of operation and c is the speed of light. Thus, for the target frequency of interest here, $f_0 = \omega_0/2\pi = 300$ MHz, the free space wavelength $\lambda_0 = 1.0$ m; and, consequently, the effective radius of the system must be smaller than the value $r_e = 1.0/(2\pi) = 15.916$ cm $= 159.16$ mm ($r_e = 79.58$ mm) to meet this electrically small criterion. The infinitesimal electric dipole, in all of the analytic cases, is driven with a 1.0 A current across its terminals; the more realistic coax-fed monopole antenna is driven with a 1.0 W input power in all of the numerical cases.

II. Optimization Methods

The geometry of an electrically small electric dipole antenna in the presence of a multilayered metamaterial spherical shell system is shown in Fig. 1. The electrically small dipole antenna is oriented along the z-axis and is positioned at the center of a set of N concentric metamaterial spherical shells. The dipole produces the fundamental, TM_{10}, radial transverse-magnetic mode. The first interior region where the dipole is located and the region exterior to the metamaterial shells are assumed to be free space. The radius of the first spherical region is always greater than the half-length of the dipole, thus entirely covering the antenna with a free space medium. The multilayered spherical metamaterial shells are modeled as N consecutive spheres

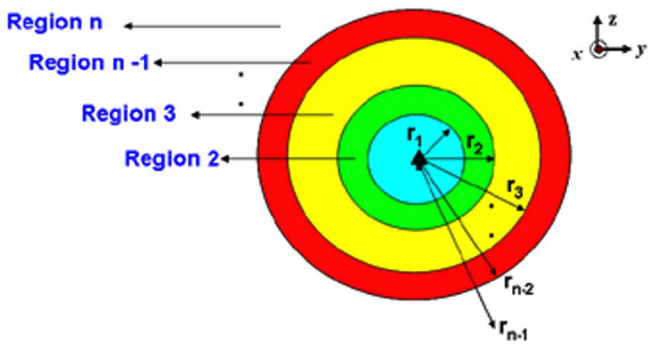

Fig. 1. Geometry of the electric dipole-multilayered metamaterial shell system centered at the origin.

with monotonically increasing radius values. The electric permittivity (ε_r) and the magnetic permeability (μ_r) of each spherical shell layer and the radius of each shell can be modeled as optimization parameters. This choice allowed the analysis of all four possible media choices, i.e., double-positive (DPS), ENG, MNG, and DNG media, for each of the metamaterial layers and spherical shell sizes.

A user friendly and robust optimization method that can calculate the optimum spherical shell radius size(s) and/or the medium parameter(s) for each metamaterial shell that will generate the maximum far-field radiated power is desired. The optimization of such a multilayer metamaterial shell system, however, proved to be a difficult task due to the extremely large E- and H-field changes which occur at the metamaterial shell boundaries, e.g., at the DPS-SNG or DPS-DNG interfaces. It has already been demonstrated that these high E- and H-field changes across these boundaries can indeed lead to unusual performance characteristics of these systems [34]. The optimization of a multiparameter EM problem is highly nonlinear and requires a robust method that will produce global maxima. One of the most well known and user friendly optimization package is provided by the MATLAB optimization toolbox. The MATLAB optimization package, however, provides only local optimization methods with the final optimization values depending on the initial guesses of the solution vector. It also requires the user to supply the possible solution parameter ranges, including both their lower and upper boundaries.

A. Genetic Algorithm

The MATLAB optimization package would be a perfect fit to accomplish our goal if it were possible to determine the solution boundary constraints prior to the MATLAB optimization cycles. GAs provide an effective alternative. They are stochastic optimization techniques based on the genetic principles of natural selection and evolution theory [44]. They use a fitness function to relate the physical problem of interest to a GA and examine the survival chances of the possible solutions in the evaluation process. The GA optimization process begins with a random initialization of the potential solutions to create the problem space. The populations of the chromosomes, a potential solution for the optimization problem using a string of optimization parameters

specified by the design problem, are evaluated with the user defined fitness function. The better-fit individuals identified in this process survive for the next generation. An optimization scheme that uses massive population sizes in principle could provide the general behavior of a metamaterial-based antenna-shell system for a large variety of possible solution parameters. The GA optimization results thus represent one possible solution for the need to obtain desirable upper and lower bounds on the solution parameters which could then be used to calculate the maximum far-field radiated power using the MATLAB optimization package.

The GA library is obtained from [45], a public-domain site that provides GA algorithm tools which can be used to build an optimization program. The GA library includes many C++ based algorithms that perform a general variety of optimization schemes using various representation and genetic operators. This present research effort did not include the development of new GA algorithms, but rather it relied on the utilization of existing GA techniques to obtain accurate solution space boundaries. The developed GA optimization algorithm was thus limited to the routines already available at the GA library website. A detailed efficiency and CPU time analysis of the algorithm strictly depends on the choice of the GA algorithm parameters; and, consequently, the overall performance of the developed algorithm was not tested. The possible solution space was created using discrete real numbers, where the number of the possible solutions, i.e., the optimization resolution, in the given solution space was set by the user.

The GA application to the metamaterial-based antenna-shell system uses several independent populations with a predetermined number of individuals that are evolved for a given generation size to obtain the maximum far-field radiated power. In each population, the optimization process is carried out separately from the other parallel populations. A crossover rate of 60% and a mutation rate of 7.5% were applied to each population. The default GA library *UniformCrossover* and *SwapMutator* tools were used to produce the children and the mutations, respectively. The best user-defined number of individuals from each population was migrated to a neighboring population providing a master population constructed with individuals from each independent population.

While the GA determines the conditions on the evolution process, it is the fitness function that selects the best individuals from each population. A fitness function that enables us to quantify the metamaterial-based antenna-shell system's far-field radiated power characteristics for different metamaterial shell sizes and medium parameter values is given below, i.e., the radiated power ratio (RPR) introduced in [35]:

$$\mathrm{RPR} = 10\ \log_{10}\left[\frac{\mathrm{P}_{\text{with shell}}(1\ \mathrm{A\ input\ current})}{P_{\text{without shell}}(1\ \mathrm{A\ input\ current})}\right]\ (\mathrm{dB}) \tag{1}$$

i.e., it is the dB value of the ratio of the total power radiated by the infinitesimal dipole antenna driven with a 1 A current in the presence of the spherical shell system to the total power radiated by the infinitesimal dipole antenna driven with a 1 A current in free space. It is also possible to use more complex fitness functions using cosine or sine functions to obtain faster convergence [46]. The RPR value is a metric that is used for the analytical solution to quantify the effect on the radiated power of the metamaterial shell when the metamaterial-based antenna is compared with the antenna itself in free space. One could compare the metamaterial-based antenna system to an antenna of the same size; but since the outer shell radius is generally only a factor of two larger than the half-length of the antenna, the RPR value would be decreased only by $\log(4) = 0.602$ dB. The RPR as defined by (1) gives a one-to-one comparison between the metamaterial-based and the bare antenna systems. It is noted that when additional comparisons are made, such as the quality factor of the system, the maximum radius of the system is used. This eliminates any advantages of the metamaterial-based antenna system that could arise from its size. It is also noted that in all of the cases discussed in this paper, the same electrical-sized system with the metamaterial shell replaced by a DPS medium was also tested; and no resonance effects were found.

We first considered a known three-layered, DPS-ENG-DPS, spherical shell system that was introduced in [35] to study how the GA library tools affect the performance of the optimization process. The metamaterial shell system consisted of three concentric spherical shells for which the first and third regions were taken to be free space, i.e., the overall system was effectively a single spherical metamaterial shell. The second region was assigned as an ENG medium with a relative permittivity that was optimized to obtain the maximum total radiated power. The relative magnetic permeability of each region was assumed to be that of free space, i.e., in every region $\mu_r = 1$. The inner and outer radius values of the system were set to 10 mm and 18.79 mm, respectively. The driving frequency of the antenna was taken to be $f_0 = 300$ MHz. The total length of the dipole was assumed to be $l = 10.0\ \mathrm{mm} = \lambda_0/100$. The relative permittivity of the ENG medium was assumed to be idealized, i.e., homogeneous and frequency independent. Thus the ENG region was first treated as a nondispersive, homogeneous layer.

A survey of the different numerical results suggested that the GA global maxima value is most sensitive to the initial discrete parameter resolution and the number of parallel populations. The solution space for the permittivity in the ENG medium was created between 0 and -10 using 0.0001 incremental steps, and massive parallel population numbers were enforced to determine the possible global maxima range. The final optimization scheme included 150 populations with 200 individuals in each population that were evolved for 300 generations.

Our goal of finding an appropriate solution space for the MATLAB optimization package using the GA-based optimization method produced a completely different radiation result that was at least 10 dB larger than the previously published maximum RPR value [35]. This promising result confirmed the first step in our hybrid optimization method, i.e., the optimized relative epsilon value was first roughly calculated with the GA method for a limited resolution. The optimized relative permittivity value was then used to create a solution space for the MATLAB optimization algorithm. It is, of course, possible to use only a GA-based optimization method to obtain a global maximum. Unfortunately, the antenna-metamaterial shell system solution process becomes very complicated for problems including many regions; and in this case, the GA method

will not satisfy our initial goal of developing a user-friendly N-region optimization method.

B. MATLAB Optimization Toolbox

The MATLAB Optimization Toolbox provides tools for general and large-scale optimization problems including minimization, equation solving, and solving least-squares or data-fitting problems. These functions all require a MATLAB m-file that contains the fitness function for the optimization problem. The MATLAB optimization toolbox provides local optimization methods; and, thus, the final optimization values depend on the initial solution vector and the solution space of the optimization problem. Since the optimization routine makes better decisions regarding step size than in an unconstrained case, an optimization design problem demonstrates better convergence behavior with well-defined constraints. [47]. The MATLAB optimization package does not require any knowledge of specific optimization methods. It is robust enough to provide accurate global maxima for well-defined lower and upper bounds of the solution space.

The constraint minimization function, *fmincon*, computes the constraint minimum of a scalar function of several optimization variables starting at an initial estimate for each optimization variable. The general definition of the *fmincon* function is shown with the following notation:

$$x = \text{fmincon}(\text{objective function}, x_0, A, b, A\text{eq}, B\text{eq}, \text{lb}, \text{ub}, \text{nonlcon}, \text{options}, P1, P2, \ldots)$$

where x_0 is the initial estimate; A and b constrain the optimization routine subject to the linear inequalities, e.g., $A \cdot x \leq b$; $A\text{eq}$ and $B\text{eq}$ constrain the optimization routine function subject to the linear equalities, e.g., $A\text{eq} \cdot x \leq b\text{eq}$; lb, and ub are lower and upper bounds on the design variables; noncoln defines the nonlinear inequalities $c(x)$ or equalities $c\text{eq}(x)$; options specifies the optimization parameters; and the parameters: $P1, P2, \ldots$, pass the problem-dependent parameters to the fitness function. The optimization variables of the antenna-metamaterial-based shell system, the medium parameters and the shell sizes, do not depend on linear or nonlinear equalities. The fmincon definition thus requires only the initial estimate for the optimization parameters and the boundary limitations of the solution space. The initial estimate of the optimization parameters were randomly assigned to provide a nonbiased optimization cycle. The upper and lower limitations of the solution space were defined by using a previously determined solution space. The GA-based global maxima values always produced results that were between 0 and -1 for a large variety of multilayered geometries. The optimization routines were supplied with a function $-f$, where f is the function being minimized, and the same fitness function given in (1) was used to evaluate the performance of the system.

The GA-MATLAB hybrid optimization algorithm was first tested with our initial 3 region, dispersionless ENG medium, benchmark problem discussed above in Section II-A. The MATLAB optimization routine produced a global maxima at 300 MHz, and the optimized relative permittivity was equal to $\varepsilon_r = -0.3389713$. The Brute-force numerical results that were published earlier estimated the relative permittivity result as $\varepsilon_r = -3.0$. These original results assumed a value of the negative permittivity and the interior radius of the ENG shell, while the outer shell radius was allowed to vary. Moreover, in the original analyses it was generally assumed that $\varepsilon_r \leq -1$. The original total radiated power value reported in [35] is 15 dB smaller than the RPR value calculated here by the MATLAB optimization routine, 77.17 dB, which identified the larger, but still negative, relative permittivity value as the best one.

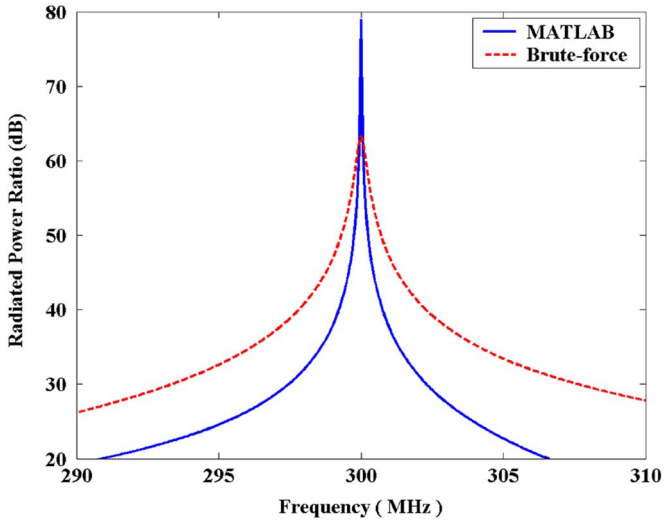

Fig. 2. RPR values as functions of the source frequency obtained using the MATLAB and the Brute-force optimization models for a $l = 10$ mm infinitesimal electric dipole in a resonant, lossless dispersive ENG shell with $r_1 = 10$ mm and $r_2 = 18.79$ mm.

With the optimized relative permittivity value determined at the target frequency, the well known Drude dispersion model was incorporated into the analysis routine to obtain the corresponding RPR values at different frequencies. A lossy Drude behavior is given by the expression

$$\varepsilon(\omega) = \varepsilon_0 \left[1 - \frac{\omega_p^2}{\omega(\omega - j\Gamma)}\right] \tag{2}$$

where ω_p is the plasma frequency and Γ is the collision frequency. When the Drude medium is lossless, $\Gamma = 0$, the permittivity crosses zero at the angular frequency $\omega = \omega_p$. The target frequency of the antenna-metamaterial-based shell system was 300 MHz, giving $\omega_0 = 2\pi \times 300$ MHz. Using a lossless Drude ENG shell with $r_1 = 10$ mm and $r_2 = 18.79$ mm and with $\omega_p = 1.3389713\,\omega_0 (\omega_p = 4\omega_0)$ to give $\text{Re}[\varepsilon_r(\omega_0)] = -0.3389713 (\text{Re}[\varepsilon_r(\omega_0)] = -3)$, the RPR values were computed with the MATLAB (the Brute-force) method. These RPR values are shown in Fig. 2. The MATLAB optimization RPR values were found to be larger and more narrowband than the Brute-force generated values. The E- and H- field distributions for these systems are compared in Fig. 3. The MATLAB optimization results produced a different fundamental radiation mode that has a much different near-field structure than was obtained with the earlier published Brute-force results [35]. While both approaches identified a resonant dipolar form of the near field distributions, the E-field and H-field distributions of the optimization-identified (brute force)

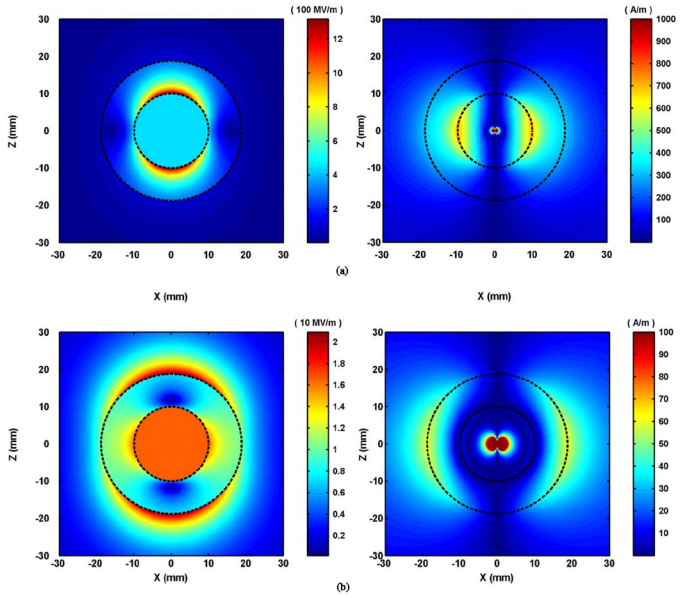

Fig. 3. Comparison of the resonant electric and magnetic field distributions generated at 300 MHz with the (a) MATLAB and the (b) Brute-force optimization methods for a $l = 10$ mm infinitesimal electric dipole in the lossless dispersive ENG shell with $r_1 = 10$ mm and $r_2 = 18.79$ mm.

case were significantly larger at the inner (outer) DPS-ENG interface. Moreover, the E-field distribution broadside to the antenna had much less amplitude in the ENG shell region for the optimization-identified resonance than it did in the brute force case. The shift of the larger E- and H-fields to the smaller radius inner DPS-ENG interface is immediately correlated with the narrower bandwidth of the RPR values. These RPR values are simply more sensitive to the source wavelengths when the inner radius is emphasized.

III. Five Region (Three-Layer Metamaterial Shell) Antenna System

An electrically small electric dipole-multilayered ENG shell system is an important example for which a robust optimization method can play a significant role in the calculation of the optimum metamaterial shell sizes and permittivity values that will produce its maximum RPR value. We considered one possible application scenario with a five region, 3 metamaterial layer, problem for which the first and fifth regions were taken to be free space and the second and fourth regions were taken to be glass layers with a relative permittivity of $\varepsilon_r = 2.25$. The third region was treated first as a hypothetical dispersionless ENG medium, where its relative permittivity was assumed to be homogeneous and to be frequency independent with a value $\varepsilon_r = -10.0$. The relative magnetic permeability of each region was assumed to be that of free space, i.e., $\mu_r = 1$. The driving frequency of the antenna was taken to be 300 MHz and the total length of the dipole was again $l = \lambda_0/100 = 10$ mm. To achieve such a value of the relative permittivity in region 3, we considered it to be filled with a cold plasma. Setting the collision frequency $\Gamma = \xi\omega_0$, the plasma density required to produce a specific relative permittivity at the target frequency was

$$N_e = 3.1437 \times 10^{-10}[1 - \varepsilon_{r,\mathrm{real}}(\omega_0)](1 + \xi^2)\omega_0^2. \quad (3)$$

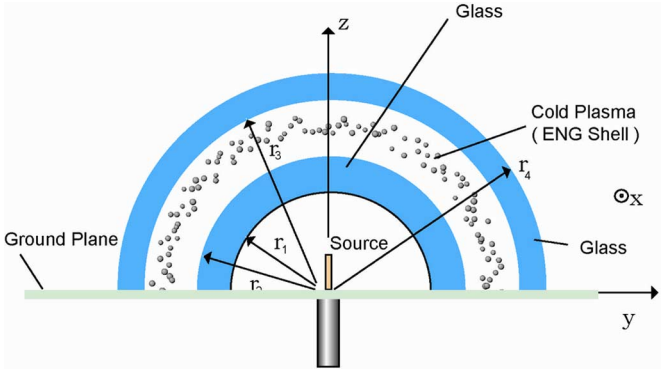

Fig. 4. Geometry of the coax-fed monopole-(glass-ENG-glass) shell system.

The desired relative epsilon value in region 3, $\varepsilon_{r,\mathrm{real}}(\omega_0) = -10.0$, can be obtained if a lossless plasma ($\xi = 0$) were contained between the glass layers that has the plasma density $N_{e,\mathrm{res}} = 1.229 \times 10^{+10}$ cm^{-3}. This plasma density is typical of the gases contained in fluorescent light bulbs. The optimization routine was then used to calculate the required ENG shell thickness that produced the maximum total radiated power. The final optimization configuration utilized the values: $r_1 = 8$ mm, $r_2 = 9$ mm, $r_3 = (\text{optimization parameter} - 1\ \text{mm})$ and $r_4 = (\text{optimization parameter})$. Thus the thickness of each glass layer was set to 1 mm; and this value was fixed in the optimization routine. The solution space for the optimization parameter was constrained between 10 mm and 20 mm. The optimized outer shell radius was $r_4 = 11.926569$ mm; the resulting configuration produced a RPR value of 74.598 dB.

A possible physical realization scenario corresponding to this analytical 5 region (DPS-ENG-DPS shell)-antenna system is shown in Fig. 4. The antenna is a coax-fed monopole in the presence of a PEC ground plane that is enclosed with a DPS-ENG-DPS hemispherical shell system. A finite element model of this system was constructed. The HFSS simulation tool was used to verify the accuracy of the analytical optimization result and to explore the radiation behavior of the system with a finite radius antenna. The length and radius of the coax-fed, thin cylindrical PEC monopole antenna were set to $a = 0.1$ mm and $l = \lambda_0/200 = 5$ mm, respectively. The HFSS simulation results were monitored through the relative radiated power gain

$$\mathrm{RPG} = 10\log_{10}\left[\frac{\mathrm{P}_{\text{with shell}}(1\ \mathrm{W\ input})}{P_{\text{without shell}}(1\ \mathrm{W\ input})}\right]\ (\mathrm{dB}). \quad (4)$$

We note that a HFSS predicted RPG value is the true relative gain and was achieved by feeding the monopole antenna with a 1 W wave-port source. The RPG values thus reflect the presence of the input impedance mismatch and the radiation efficiency of the system. Hence, it represents the overall efficiency of the system. The RPG values are different from the RPR values because the analytical model does not include the input impedance mismatch or the physical effects of the size of the antenna and its feedline. The HFSS coax-fed monopole-multilayered hemispherical model was also defined with $r_1 = 8$ mm, $r_2 = 9$ mm, and $r_3 = r_4 - 1$ mm and with $\varepsilon_{2r} = \varepsilon_{4r} = 2.25$ and $\varepsilon_{3r,\mathrm{real}}(\omega_0) = -10.0$. By varying the outer radius, r_4, the HFSS model produced a maximum RPG = 70.34 dB at $r_4 = 11.909$ mm. The slight difference between the numerical

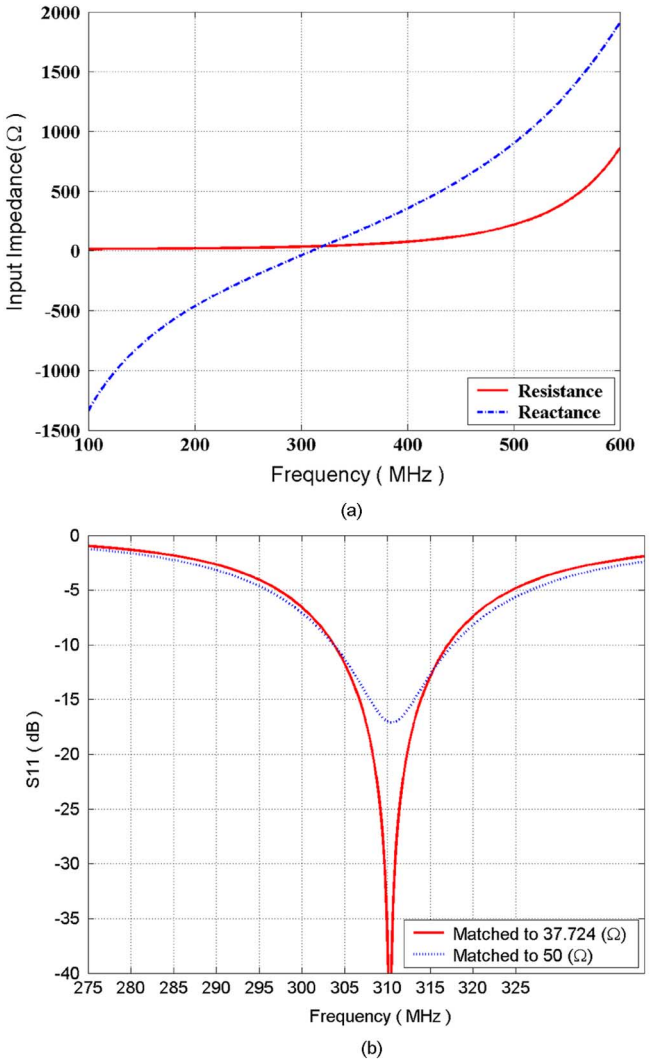

Fig. 5. (a) Complex input impedance and (b) S_{11} values for the matched, resonant, electrically-small coax-fed monopole-(glass-ENG-glass) shell system as functions of the source frequency. The ENG shell was modeled as a hypothetical frequency-independent medium.

and the analytical solution values of r_4 is due to the finite capacitance introduced by the coax-fed monopole antenna, i.e., the ENG shell thickness must be adjusted to account for this additional capacitance. The monopole antenna-multilayered shell system parameters were then further optimized to improve the overall efficiency of the entire antenna system. A coax-fed monopole-glass-ENG-glass shell system that was matched to a 50 Ω input source was finally obtained. It is defined by the following dimensions: monopole antenna length $= 4.1$ mm, monopole antenna radius $= 0.6$ mm and $r_4 = 11.928$ mm. The complex input impedance values of the overall system at 300 and 310 MHz were $Z_{in} = 35.15 - j \times 38.38\ \Omega$ and $Z_{in} = 37.724\ \Omega$, respectively.

Fig. 5 shows the complex input impedance and the S_{11} values of the final optimized electrically small coax-fed monopole antenna-(glass-ENG-glass) shells system for 37.724 and 50 Ω source impedances. This optimized configuration produces a resonant antenna response at $f_{res} = 310.26$ MHz that results in a 98.04% (99.99%) overall efficiency for the 50 Ω (37.724 Ω) source. Using the HFSS predicted frequency-dependent input impedance values and [16, Eq. (86)], the calculated Q value for this hypothetical frequency-independent ENG shell-based antenna system at 310.26 MHz was 15.516, significantly below the Chu limit value [11]

$$Q_{\text{Chu}} = \frac{1}{(k_0 r_4)^3} + \frac{1}{k_0 r_4} = 2389. \tag{5}$$

Using the axi-symmetric finite element software tool in the COMSOL Multiphysics package [48], we were able to resolve the problem sufficiently to include dispersive effects in the ENG shell. The finer resolution required a slight modification in the geometry to achieve similar operating characteristics. In particular, with the same coax feed but with the monopole length being $\ell = 4.064$ mm; with the radii: $r_1 = 8$ mm, $r_2 = 9$ mm, and $r_3 = 10.979$ mm and $r_4 = 11.979$ mm; and with the relative permittivities: $\varepsilon_{2r} = \varepsilon_{4r} = 2.25$ and $\varepsilon_{3r} = -10.0$, the resonance frequency for this frequency-independent ENG shell case was found to be $f_{res} = 310.45$ MHz; and the input impedance at that frequency was $Z_{in} = 40.76 + j \times 0.005\ \Omega$, giving an overall efficiency equal to 98.97%. This configuration had $k_{res} r_4 = 0.0727$ and, hence, the ideal Q value was $Q_{\text{Chu}} = 2616$. Again, the actual Q value was obtained with the calculated input impedance values and (86) from [16]. For this frequency-independent case the Q value was 15.97, in very good agreement with the HFSS predicted value. A lossless Drude model

$$\varepsilon_r(\omega) = 1.0 - 11(\omega_{\text{res}}/\omega)^2 \tag{6}$$

was then introduced to describe the ENG shell as a dispersive medium. It was designed to give $\varepsilon_{3r,\text{real}}(\omega_{\text{res}}) = -10.0$ and, consequently, the same overall efficiency at the resonance frequency. However, because the numerical model could now resolve, in the presence of dispersion, the frequency behavior of the input impedance near the resonance frequency, the corresponding Q value could be determined accurately. It was found that the Q value increased significantly to 4563 at this resonance frequency, 1.74 times larger than the Chu value. On the other hand, to understand the potential bandwidth properties of this system, the lossless dispersion model

$$\varepsilon_r(\omega) = 1.0 - 11(\omega_{\text{res}}/\omega)^{10/11} \tag{7}$$

was also used to model the ENG shell and produce the same high overall efficiency. Near the resonance frequency this dispersion model satisfies the limiting behavior given by [49, (2.38)], the Entropy condition

$$\partial_\omega(\omega\varepsilon_r) \geq 0 \tag{8}$$

This condition follows from the requirement that the value of the electric field energy be positive definite. The Q value obtained with the ENG shell described by this dispersion-limit model was

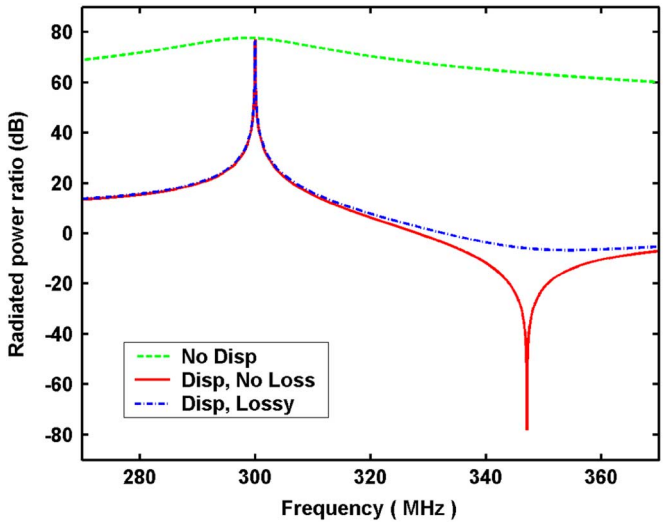

Fig. 6. RPR values as a function of the source frequency for a $l = 10$ mm infinitesimal electric dipole enclosed in a single ENG shell whose radii: $r_1 = 10$ mm and $r_2 = 18.79$ mm. The permittivity of the ENG shell is described by a frequency independent model, a lossless Drude model, and a lossy Drude model.

only 2080, 0.79 times smaller than the Chu value. These dispersion-based results are in good agreement with those discussed in [35] and [50].

IV. Single and MultiBand Electrically-Small Electric Dipole-Multilayered Metamaterial-Based Spherical Shell Designs

Advances in technology will continue to require smaller circuitry to further reduce the overall size of current wireless communication and sensor systems. One approach to achieve this reduction in size is to develop small, efficient and multiband structures that will fit into restricted areas while simultaneously accommodating the desired frequencies and high data rates. The design of electrically small, high density systems is a difficult task due to the large coupling that exists between the individual radiating elements in the system when they are in close proximity to each other. This coupling changes both the field distributions and input impedances of each radiating element.

Consider again the optimized infinitesimal dipole-single ENG shell system, but now with the ENG region described by the lossless and the lossy Drude models. The RPR values for this system when the ENG shell is described with the frequency independent value $\varepsilon_r = -0.3389713$, with a lossless Drude model ($\Gamma = 0$) having $\varepsilon_r(\omega_0) = -0.3389713$, and with a lossy Drude model having $\Gamma = 10^{-5}\,\omega_0$ while maintaining $\mathrm{Re}[\varepsilon_r(\omega_0)] = -0.3389713$, are shown in Fig. 6 as a function of the source frequency. Fig. 6 demonstrates that these systems are resonant and achieve their peak RPR values at the target frequency. However, it also shows that for a particular frequency, $f_{\mathrm{NR}} = 347.1377$ MHz, the system is essentially nonradiating (NR). The RPR value at $f_{\mathrm{NR}} = 347.1377$ MHz is -78.19 dB. The appearance of this NR behavior of this antenna system is a natural consequence of the dispersion effects introduced by the Drude model for the permittivity in region 3. Because the source frequency approaches the plasma frequency as it increases, the relative permittivity value in the lossless case at the NR frequency is nearly zero, i.e., $\varepsilon_r(\omega_{\mathrm{NR}}) = 2.352 \times 10^{-5} \approx 0$. This near zero permittivity causes the NR mode. Similarly, even though the lossy Drude case has an RPR value smaller than one (~ -6 dB) at the NR frequency, it does not exhibit the extremely small value obtained in the lossless Drude case. The presence of even a very small amount of loss is enough to move the relative permittivity value sufficiently away from zero, which detunes this NR mode. We note that the frequency of the NR mode can be shifted to any desired source frequency, such as 300 MHz, by simply moving the zero crossing of the relative permittivity to that frequency value. This is effectively achieved by modifying the plasma frequency appropriately. A comparison of the frequency independent permittivity results and those obtained with the frequency dispersive ENG models show that dispersion significantly impacts that bandwidth performance of the system in agreement with previous observations of this effect [35]–[38]. We note that while the introduction of losses impacted the NR mode, the effect on the radiating mode was significantly less.

Fig. 7 shows the E- and H-field distributions of the NR mode at 347.1377 MHz for the optimized infinitesimal dipole-single ENG spherical shell system. A comparison of these NR E- and H-field distributions and the ones associated with the radiating modes shown in Fig. 3 reveals several interesting behaviors. In both cases, it is clear that the dipole mode is dominating the behavior. Moreover, both the electric and magnetic fields have large values that are concentrated across the ENG shell interfaces. In the strongly radiating case one finds that the electric field in the interior sphere, the free-space region that surrounds the anntena, is uniform and large. In contrast, while the electric field in the interior sphere is also uniform in the NR mode, its magnitude is nearly equal to zero. The electric field basically becomes confined to the ENG shell in the NR mode. On the other hand, the magnetic field becomes localized within the interior shell. Additionally, the maximum electric and magnetic field strengths are orthogonal to each other. Thus there is an effective decoupling of the electric and magnetic fields and this causes the NR state of the system. Extensive numerical studies suggest that indeed the main cause for this unique NR mode is having the relative permittivity value close to zero with either a positive or negative real value. The resonant antenna-metamaterial shell models have been shown to be sensitive [35] to changes in the geometry and medium parameters. Without the guidance obtained from the optimization approach to explore values of the relative permittivity in the $(-1, 0]$ range in the presence of dispersion, such as the Drude model, these NR modes would not have been identified. The NR mode reported here was not noticed in our earlier studies [35] due to the use of frequency independent material models and an emphasis on relative permittivity values smaller than -1.

The desire for multiband radiating and nonradiating antenna designs is another well-suited problem for the hybrid optimization model introduced here. In particular, the medium characteristics of a specified number of shells and their thicknesses can be optimized to achieve a maximum or minimum RPR value at some set of source frequencies. For example, we have considered another five region problem where the inner shell radius

TABLE I
OPTIMIZED PERMITTIVITY VALUES OF THE MULTILAYERED METAMATERIAL SHELL MODEL

	r_1 (mm)	r_2 (mm)	r_3 (mm)	r_4 (mm)	Region 2 (ε_r)	Region 3 (ε_r)	Region 4 (ε_r)
RPR Max at 300 MHz	8	9	10	11	-0.106	-0.415	-0.574
NR feature at 300 MHz	8	9	10	11	-9.97×10^{-5}	-0.415	-0.574

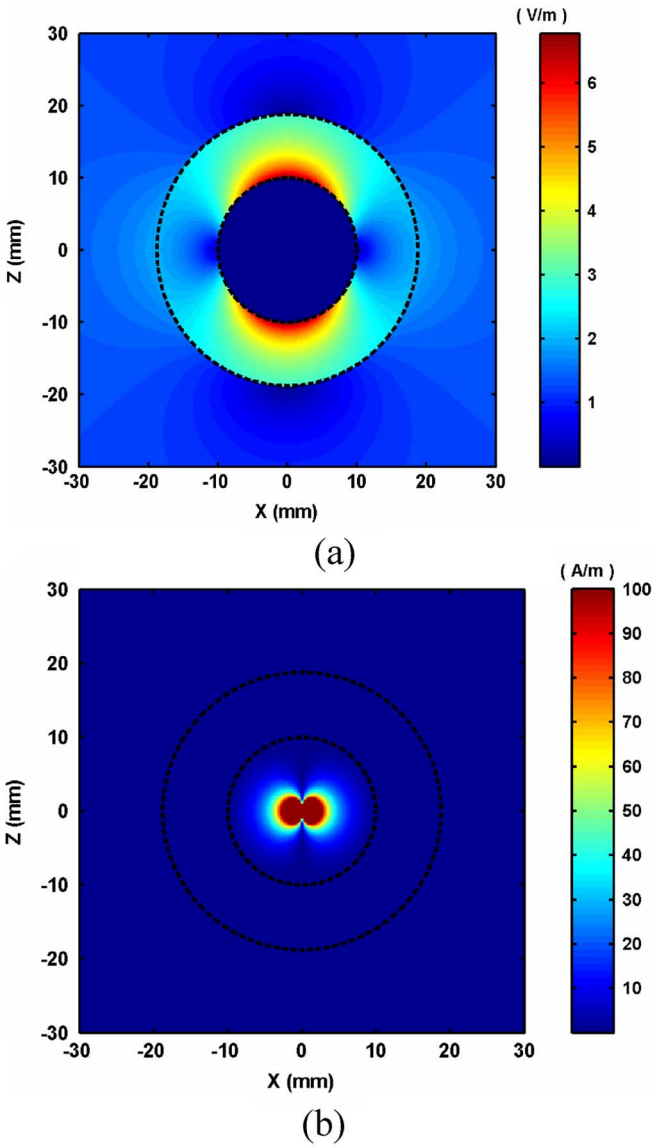

Fig. 7. The behavior of the NR mode at 347.1377 MHz. (a) E-field distribution and (b) H-field distribution.

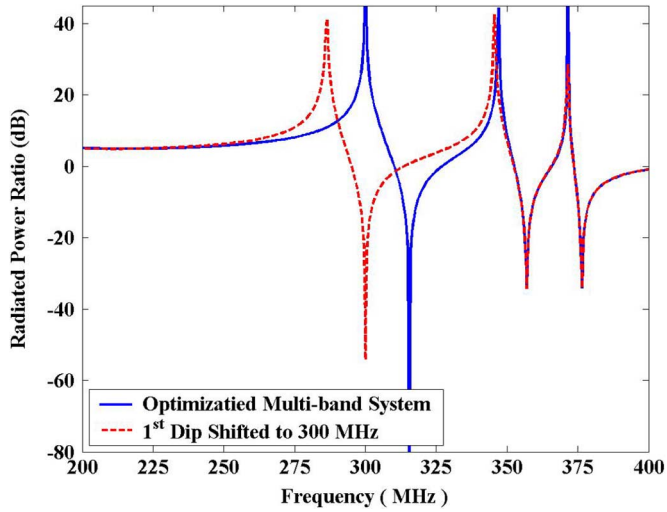

Fig. 8. Optimized RPR values for a $l = 10$ mm infinitesimal electric dipole in a five region, 3 layer dispersive ENG shell system. (a) Optimized multiband result with the first RPR maximum at 300 MHz and (b) optimized multiband result with first NR feature at 300 MHz.

was set to $r_1 = 8$ mm and the thickness of each of the spherical shell layers were fixed to be 1 mm. The first and fifth regions were again taken to be free space. The relative permeability of each region was assumed to be that of free space, i.e., $\mu_r = 1$. The driving frequency of the antenna was taken to be 300 MHz, and the total length of the dipole was set to be $l = \lambda_0/100 = 10$ mm. The relative permittivity values of the second, third and fourth regions were assigned as optimization parameters, and the corresponding lower and upper solution space boundaries were set to $[-1e-5, -0.2]$, $[-0.2, -1]$, and $[-0.2, -1]$, respectively. This infinitesimal dipole antenna-multilayered metamaterial shell configuration was then optimized first to achieve a maximum RPR value at 300 MHz. Since we now know that a NR feature will appear at a frequency above the radiating mode resonant frequency (near to where the permittivity approaches zero), it was then also straightforward to shift this minimum RPR value to 300 MHz with a related choice of the permittivity values. Plots of the RPR values as a function of the frequency including the lossless Drude model for the dispersion of each region for these two cases, one with the first radiating mode feature and one with the first NR mode feature appearing at 300 MHz, are given in Fig. 8. The relative permittivity values corresponding to these two cases are summarized in Table I. As described in Section II, the first NR RPR feature, again, can be judiciously shifted to the desired operation frequency. The other two nonradiating modes may be relocated by using either a separate optimization problem emphasizing the frequency region of interest or simply the Brute-force method. The NR modes for the optimized maximum RPR case occur at 315.48, 356.95, and 376.49 MHz, respectively. The E-field distributions of the infinitesimal electric dipole-multilayered spherical shell system for all of these NR modes are shown in Fig. 9. We find that the NR E- and H-field distributions have essentially the same character at all of these frequencies, i.e., the electric field is concentrated in an ENG layer and the magnetic field is concentrated in the core region. However,

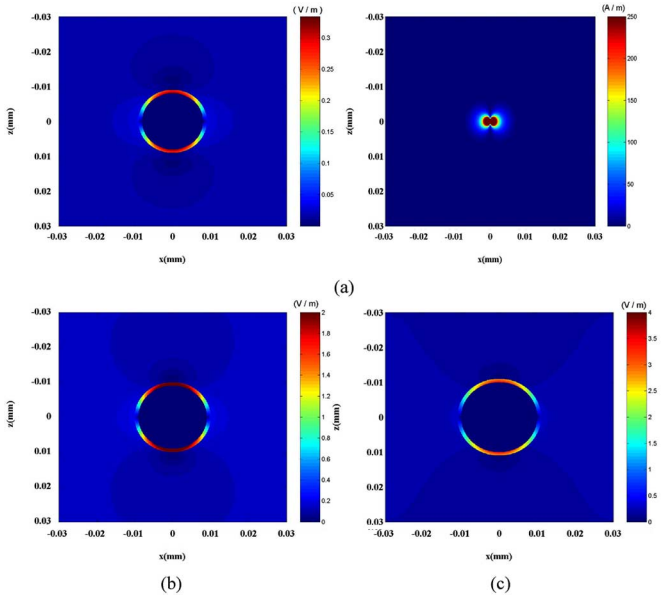

Fig. 9. The NR mode field distributions for the infinitesimal dipole-3 multilayer ENG shell system that has its RPR maximized at 300 MHz. (a) E- and H-field distributions at 315.48 MHz, (b) E-field distribution at 356.95 MHz, and (c) E-field distribution at 376.49 MHz.

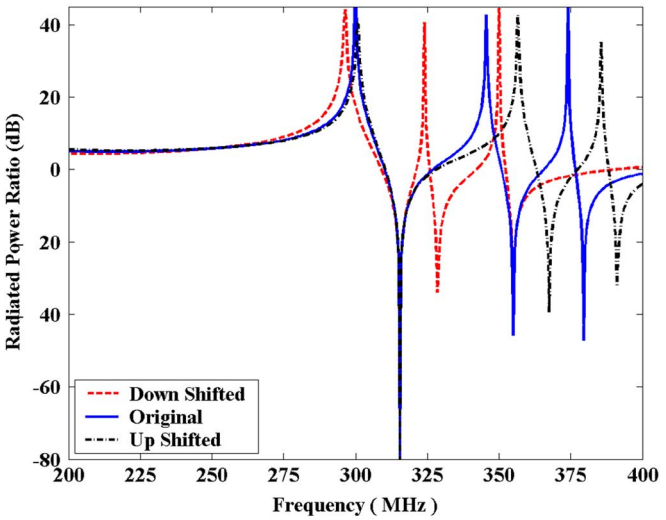

Fig. 10. The locations of the radiating and nonradiating resonant modes of an infinitely small electric dipole in a three-layer Drude dispersive ENG shell system can be shifted to any desired frequency in a specified frequency band of interest using the Brute-force optimization approach.

one finds that only one of the layers will capture the NR electric field distribution for a given frequency, and thus each of the NR modes corresponds to a different layer. The frequencies at which the NR modes appear for the corresponding specified NR location case are 300, 356.95, and 376.49 MHz, respectively. The locations of the second and third NR features in this case were designed to be at the same frequencies as the NR modes in the peak-RPR-at-300 MHz case. We have found that n maximum RPR and, hence, n NR features can be obtained with an n-multilayered system. The first n nonradiating RPR null features are produced by the corresponding n near-to-zero relative epsilon values in the n-layered metamaterial shell system. The first NR mode is the result of the smallest relative epsilon value in the system. The relative permittivity values associated with the next two NR modes have slightly increasing plasma frequency values. The E-field distributions for thicker shell sizes are slightly more complicated and are discussed further in [51].

The capability to target the frequencies at which the radiating or nonradiating modes occur is simply accomplished using the Brute-force optimization approach. The radiating (nonradiating) maxima (minima) locations are adjusted by changing the relative epsilon values that correspond to the maxima (minima) of the RPR results. For example, the NR second and third modes can be shifted to lower (higher) frequencies by reducing (increasing) the corresponding plasma frequency, hence, the corresponding relative permittivity value in the different layers. Fig. 10 demonstrates our capability of up and down shifting the frequency locations of the RPR responses in a given frequency window. This also demonstrates our ability to optimize the locations of the resonant radiating and nonradiating modes for multiband operation in a specified frequency interval.

V. Conclusion

An electrically small electric dipole antenna in the presence of a multilayered metamaterial shell system was developed analytically and the total radiated power of this system was optimized using a hybrid GA-MATLAB optimization approach. The GA optimization results were used to obtain the upper and lower solution space bounds that were required to calculate the maximum total radiated power using the MATLAB optimization package. The numerical studies demonstrated that the GA global maxima value is most sensitive to the initial discrete parameter resolution and the number of parallel populations. While it would also be possible to use only a GA-based optimization method to obtain a global maximum, the analytical solutions for the N-layer metamaterial shell system, when N gets large, become much more complicated. The MATLAB toolset provides a simpler optimization approach for this more complicated antenna problem.

The MATLAB optimization model produced a global maximum that is 15 dB larger than the earlier published Brute-force method results at 300 MHz. In particular, they revealed the advantages of exploiting the $(-1, 0)$ relative permittivity (permeability) regime. Comparisons of the total radiated power results and the electric and magnetic field distributions generated by the system parameters identified by the MATLAB and Brute-force models also revealed both radiating and nonradiating modes, further proving the importance of the optimization model. A specific application of the optimization model to the analytical solution of the dipole-N-layer metamaterial spherical shell system was considered. Particular emphasis was given to a spherical glass shell filled with a "cold plasma" medium at 300 MHz. Both analytical and HFSS numerical models were considered. An electrically small coax-fed monopole antenna-(glass-ENG-glass) hemispherical shell system was also constructed and simulated numerically with a three-dimensional ANSOFT HFSS model and a two-dimensional COMSOL Multiphysics axi-symmetric model. The ENG shell was treated as a dispersive medium in the analytical and COMSOL Multiphysics models; it was treated as a frequency-independent medium in the HFSS

models. The analytical optimization, ANSOFT HFSS, and COMSOL Multiphysics simulation results showed very good agreement for the frequency-independent ENG shell cases. It was further demonstrated with the ANSOFT HFSS and COMSOL Multiphysics models that this optimization-inspired configuration produces a resonant antenna response (a total input reactance equal to zero and a matched input resistance) that resulted, respectively, in a 98.04% overall efficiency at 310.26 MHz and a 98.97% overall efficiency at 310.45 MHz for a 50 Ω source. The COMSOL Multiphysics calculated Q value for this antenna system at the resonance frequency, 310.45 MHz, for the assumed hypothetical frequency-independent homogenous ENG medium, was 15.97 for $k_{\rm res}r_4 = 0.0727$, significantly below 2616, the Chu limit value. The COMSOL Multiphysics models that treated the ENG shell as a lossless dispersive medium predicted the same overall efficiencies, but significantly larger Q values. With a Drude dispersion model, the Q value at this resonance frequency was 4563, 1.74 times larger than the Chu value. With a dispersion-limit model, it was 2080, 0.79 times smaller than the Chu value. These results are in good agreement with related considerations reported elsewhere [50] of the impact of dispersion on the Q values of these electrically-small resonant systems.

Finally, a multiband radiating or nonradiating antenna design was considered using the developed hybrid optimization model. A five region, 3-layer dispersive spherical ENG shell system was studied to understand the general radiation behavior of these systems. The optimization results revealed that an N-layer shell system can be designed to support N radiating and N nonradiating resonant modes. The RPR and field distribution results for the 3-layer problem revealed the behavior of the location of the frequencies of these radiating and nonradiating modes. It was demonstrated that the NR mode locations were associated with the near-zero permittivity values obtained through the Drude model behavior in each layer. The magnetic field distributions of the NR modes are concentrated in the interior sphere; the corresponding electric field distributions are concentrated in the layer having the near-zero permittivity value. This decoupling of the electric and magnetic field behavior is responsible for the NR mode. It was also shown that the frequency locations of the NR modes for a multiband system can be shifted to lower or higher frequencies by reducing or increasing the corresponding plasma frequency and, hence, relative permittivity values of the layers.

We are currently exploring systems in which one can exploit these nonradiating modes. In particular, as will be shown elsewhere, the coupling between two closely spaced electrically small radiating elements can be reduced significantly by placing an electrically small NR sphere between them. Ultra-dense arrays of resonantly-enhanced metamaterial-based radiating elements can be achieved with these interspersed NR spheres; these results will be reported elsewhere.

REFERENCES

[1] L. J. Chu, "Physical limitations of omnidirectional antennas," *J. Appl. Phys.*, vol. 19, pp. 1163–1175, Dec. 1948.

[2] H. A. Wheeler, "Fundamental limitations of small antennas," *IRE Proc.*, vol. 35, pp. 1479–1484, Dec. 1947.

[3] H. A. Wheeler, "The radiansphere around a small antenna," *IRE Proc.*, vol. 47, pp. 1325–1331, Aug. 1959.

[4] R. E. Collin and S. Rothschild, "Evaluation of antenna Q," *IEEE Trans. Antennas Propag.*, vol. AP-12, no. 1, pp. 23–27, Jan. 1964.

[5] R. L. Fante, "Quality factor of general ideal antennas," *IEEE Trans. Antennas Propag.*, vol. AP-17, no. 3, pp. 151–155, Mar. 1969.

[6] H. A. Wheeler, "Small antennas," *IEEE. Trans. Antennas Propag.*, vol. AP-23, Jul. 1975.

[7] E. H. Newman, P. Bohley, and C. H. Walter, "Two methods for the measurement of antenna efficiency," *IEEE Trans. Antennas Propag.*, vol. AP-23, no. 4, pp. 457–461, Jul. 1975.

[8] G. S. Smith, "Efficiency of electrically small antennas combined with matching networks," *IEEE Trans. Antennas Propag.*, vol. AP-40, no. 5, pp. 369–373, May 1977.

[9] R. C. Hansen, "Fundamental limitations in antennas," *Proc. IEEE*, vol. 69, pp. 170–181, Feb. 1981.

[10] L. Fante, "Maximum possible gain for an arbitrary ideal antenna with specified quality factor," *IEEE Trans. Antennas Propag.*, vol. AP-40, no. 12, pp. 1586–1588, Dec. 1992.

[11] J. S. McLean, "A re-examination of the fundamental limits on the radiation Q of electrically small antennas," *IEEE Trans. Antennas Propag.*, vol. AP-44, pp. 672–676, May 1996.

[12] S. R. Best, "The radiation properties of electrically small folded spherical helix antennas," *IEEE Trans. Antennas Propag.*, vol. 52, no. 4, pp. 953–960, Apr. 2004.

[13] S. R. Best, "A discussion on the properties of electrically small self-resonant wire antennas," *IEEE Antennas and Propag. Mag.*, vol. 46, no. 6, pp. 9–22, Dec. 2004.

[14] S. R. Best, "A discussion on the quality factor of impedance matched electrically small wire antennas," *IEEE Trans. Antennas Propag.*, vol. 53, no. 1, pp. 502–508, Jan. 2005.

[15] S. R. Best, "Low Q electrically small linear and elliptical polarized spherical dipole antennas," *IEEE Trans. Antennas Propag.*, vol. 53, no. 3, pp. 1047–1053, Mar. 2005.

[16] A. D. Yaghjian and S. R. Best, "Impedance, bandwidth, and Q of antennas," *IEEE Trans. Antennas Propag.*, vol. 53, no. 4, pp. 1298–1324, Apr. 2005.

[17] R. P. Harrington, *Time Harmonic Electromagnetic Fields*. New York: McGraw-Hill, 1961, pp. 414–420.

[18] C. A. Balanis, *Antenna Theory*, 3rd ed. New York: Wiley, 2005, pp. 637–641.

[19] G. Skahill, R. M. Rudish, and J. Piero, "Electrically small, efficient, wide-band, low-noise antenna elements," in *Proc. Antenna Applications Symp.*, Allerton Park, Monticello, IL, Sep. 16–18, 1998, pp. 214–231.

[20] Y. Kim and D. L. Jaggard, "The fractal random array," *Proc. IEEE*, vol. 74, pp. 1278–1280, Sept. 1986.

[21] C. Puente, J. Romeu, and A. Cardama, "Fractal antennas," in *Frontiers in Electromagnetics*, D. H. Werner and R. Mittra, Eds. Piscataway, NJ: IEEE Press, 2000, pp. 48–93.

[22] D. H. Werner, R. L. Haupt, and P. L. Werner, "Fractal antenna engineering: The theory and design of fractal antenna arrays," *IEEE Antennas Propag. Mag.*, vol. 41, no. 5, pp. 37–59, Oct. 1999.

[23] D. H. Werner and S. Ganguly, "An overview of fractal antenna engineering research," *IEEE Antennas Propag. Mag.*, vol. 45, no. 1, pp. 38–56, Feb. 2003.

[24] K. J. Vinoy, K. A. Jose, V. K. Varadan, and V. V. Varadan, "Hilbert curve fractal antenna: A small resonant antenna for VHF/UHF applications," *Microw. Opt. Technol. Lett.*, vol. 29, no. 4, pp. 215–219, May 2001.

[25] S. R. Best, "A comparison of the performance properties of the Hilbert curve fractal and meander line monopole antennas," *Microw. Opt. Technol. Lett.*, vol. 35, no. 4, pp. 258–262, Nov. 2002.

[26] J. Zhu, A. Hoorfar, and N. Engheta, "Peano antennas," *IEEE Antennas Wireless Propag. Lett.*, vol. 3, pp. 71–74, 2004.

[27] J. Zhu, A. Hoorfar, and N. Engheta, "Bandwidth, cross polarization, and feed-point characteristics of matched Hilbert antennas," *IEEE Antennas Wireless Propag. Lett.*, vol. 2, pp. 2–5, 2003.

[28] E. E. Altshuler, "Electrically small self-resonant wire antennas optimized using a genetic algorithm," *IEEE Trans. Antennas Propag.*, vol. AP-50, no. 3, pp. 297–300, Mar. 2002.

[29] R. W. Ziolkowski and A. Kipple, "Application of double negative metamaterials to increase the power radiated by electrically small antennas," *IEEE Trans. Antennas Propag.*, vol. 51, no. 10, pp. 2626–2640, Oct. 2003.

[30] R. W. Ziolkowski and A. D. Kipple, "Reciprocity between the effects of resonant scattering and enhanced radiated power by electrically small antennas in the presence of nested metamaterial shells," *Phys. Rev. E.*, vol. 72, no. 036602, Sept. 2005.

[31] R. W. Ziolkowski, "Applications of metamaterials to realize efficient electrically small antennas," in *Programme and Abstracts of the EPFL LATSIS Symp.*, Lausanne, Switzerland, Feb. 28–Mar. 2 2005, pp. 65–67.
[32] R. W. Ziolkowski, "Metamaterials applications to electrically small antennas," in *Proc. IEEE Int. Workshop on Antenna Technology: Small Antennas and Novel Metamaterials*, Singapore, Mar. 7–9, 2005, pp. 7–10.
[33] R. W. Ziolkowski, " Metamaterials applications to electrically small antennas," in *Proc. Loughborough Antennas and Propagation Conf.*, Loughborough, U.K., Apr. 4–6 2005, pp. 65–67.
[34] N. Engheta and R. W. Ziolkowski, "A positive future for double negative metamaterials," *IEEE Microwave Theory Tech.*, vol. 53, no. 4, pp. 1535–1556, Apr. 2005.
[35] R. W. Ziolkowski and A. Erentok, "Metamaterial-based efficient electrically small antennas," *IEEE Trans. Antennas Propag.*, vol. 54, pp. 2113–2130, Jul. 2006.
[36] A. Erentok and R. W. Ziolkowski, "Dipole antennas enclosed in double negative (DNG) and single-negative (SNG) nested spheres: Efficient electrically small antennas," presented at the IEEE AP-S Int. Symp. and USNC/URSI National Radio Science Meeting, Washington, DC, Jul. 3–8, 2005.
[37] A. Erentok and R. W. Ziolkowski, "HFSS modeling of a dipole antenna enclosed in a an epsilon-negative (ENG) metamaterial shell," presented at the IEEE AP-S Int. Symp. and USNC/URSI National Radio Science Meeting, Washington, DC, Jul. 3–8, 2005.
[38] A. Erentok and R. W. Ziolkowski, "Metamaterial-based realizations of efficient electrically small antennas," presented at the URSI Radio Science Meeting, Session B2, Boulder, CO, Jan. 2005.
[39] H. B. Keller and J. B. Keller, "Reflection and transmission of electromagnetic waves by a spherical shell," *J. Appl. Phys.*, vol. 20, pp. 393–396, Apr. 1949.
[40] M. G. Andreasen, "Radiation from a radial dipole through a thin dielectric spherical shell," *IRE Trans. Antennas Propag.*, vol. 5, pp. 337–342, Oct. 1957.
[41] H. R. Raemer, "Radiation from linear electric or magnetic antennas surrounded by a spherical plasma shell," *IRE Trans. Antennas Propag.*, vol. 10, pp. 69–78, Jan. 1962.
[42] R. V. Row, "Radiation efficicency of electric and magnetic dipole antennas surrounded by a small spherical shell of lossy dielectric," *IEEE Trans. Antennas Propag.*, vol. 12, pp. 646–647, Sep. 1964.
[43] D. E. Burrick, "Spheres," in *Radar Cross Section Handbook*, G. T. Ruck, D. E. Barrick, W. D. Stuart, and C. K. Krichbaum, Eds. New York: Plenum Press, 1970, vol. 1, ch. 3.
[44] Y. Rahmat-Samii and E. Michielssen, *Electromagnetics Optimization by Genetic Algorithm*. New York: McGraw-Hill, 1999.
[45] [Online]. Available: http://lancet.mit.edu/ga/(03/01/2006)
[46] A. Erentok and K. L. Melde, "Comparison of MATLAB and GA optimization for three-dimensional pattern synthesis of circular arc arrays," presented at the IEEE Antennas and Propagation Society Int. Symp. and USNC/URSI National Radio Science Meeting, Session 55, Monterey, CA, Jun. 20–26, 2004.
[47] [Online]. Available: http://www.mathworks.com/(03/01/2006)
[48] [Online]. Available: http://www.comsol.com/(09/12/2006)
[49] C. Caloz and T. Itoh, *Electromagnetic Metamaterials, Transmission Line Theory and Microwave Applications*. Hoboken, NJ: Wiley, 2006.
[50] R. W. Ziolkowski and A. Erentok, "At and below the Chu limit: Passive and active broad bandwidth metamaterial-based efficient electrically small antennas," *IET Microw., Antennas, Propag.*, 2007, to be published.
[51] A. Erentok and R. W. Ziolkowski, "Multi-band non-radiating electrically small spherical shell designs," presented at the IEEE Antennas and Propagation Society Int. Symp. and USNC/URSI National Radio Science Meeting, Albuquerque, NM, Jun. 2006.

Aycan Erentok received the B.S. (*cum laude* and honors) and M.S. degrees from the University of Arizona, Tuscon, in 2001 and 2003, respectively, all in electrical engineering. He is currently a doctoral student in the Electrical and Computer Engineering Department at the University of Arizona.

His current research interests include EM optimization algorithms, electrically small antennas and effects of metamaterials on antenna performance. He holds a provisional patent issued by the University of Arizona for the physical realization of electrically-small antennas based on metamaterial-inspired structures.

Mr. Erentok received third place in the student paper competition at the 2004 URSI National Radio Science Meeting in Boulder, CO.

Richard W. Ziolkowski (M'97–SM'91–F'94) received the Sc.B. degree in physics (*magna cum laude* with honors) from Brown University, Providence, RI, in 1974 and the M.S. and Ph.D. degrees in physics from the University of Illinois at Urbana-Champaign, in 1975 and 1980, respectively.

He was a member of the Engineering Research Division at the Lawrence Livermore National Laboratory, CA, from 1981 to 1990 and served as the leader of the Computational Electronics and Electromagnetics Thrust Area for the Engineering Directorate from 1984 to 1990. He joined the Department of Electrical and Computer Engineering at the University of Arizona as an Associate Professor in 1990, and was promoted to Full Professor in 1996. He was selected by the Faculty to serve as the Kenneth Von Behren Chaired Professor for 2003–2005. He holds a joint appointment with the College of Optical Sciences at the University of Arizona. His research interests include the application of new mathematical and numerical methods to linear and nonlinear problems dealing with the interaction of acoustic and electromagnetic waves with complex media, metamaterials, and realistic structures.

Prof. Ziolkowski is a member of Tau Beta Pi, Sigma Xi, Phi Kappa Phi, the American Physical Society, the Optical Society of America, the Acoustical Society of America, and Commissions B (Fields and Waves) and D (Electronics and Photonics) of International Union of Radio Science (URSI). He is a Fellow of the Optical Society of America. He was awarded the Tau Beta Pi Professor of the Year Award in 1993 and the IEEE and Eta Kappa Nu Outstanding Teaching Award in 1993 and 1998. He served as the Vice Chairman of the 1989 IEEE/AP-S and URSI Symposium in San Jose, and as the Technical Program Chairperson for the 1998 IEEE Conference on Electromagnetic Field Computation. He served as a member of the IEEE Antennas and Propagation Society (AP-S) Administrative Committee (ADCOM) from 2000–2002. He served as the IEEE AP-S Vice President in 2004 and President in 2005. He is currently serving as a Past-President member of the AP-S ADCOM. He was a Steering Committee Member for the 2004 ESA Antenna Technology Workshop on Innovative Periodic Antennas. He served as a co-Chair of the International Advisory Committee for the inaugural IEEE International Workshop on Antenna Technology: Small Antennas and Novel Metamaterials, IWAT2005, and as a member of the International Advisory Committee for IWAT2006. He was member of the International Advisory Committee for the IEEE 2005 Int. Symp. on Microwave, Antenna, Propagation and EMC Technologies, MAPE2005. He was an Associate Editor for the IEEE TRANSACTIONS ON ANTENNAS AND PROPAGATION from 1993–1998. He was a co-Guest Editor for the October 2003 IEEE TRANSACTIONS ON ANTENNAS AND PROPAGATION Special Issue on Metamaterials. For the U.S. URSI Society he served as Secretary for Commission B (Fields and Waves) from 1993–1996 and as Chairperson of the Technical Activities Committee from 1997–1999, and as Secretary for Commission D (Electronics and Photonics) from 2001–2002. He served as a Member-at-Large of the U.S. National Committee (USNC) of URSI from 2000–2002 and is now serving as a member of the International Commission B Technical Activities Board. He was a co-Guest Editor of the 1998 special issue of *J. Opt. Soc. Am. A* featuring Mathematics and Modeling in Modern Optics. He was a co-Organizer of the Photonics Nanostructures Special Symposia at the 1998, 1999, 2000 OSA Integrated Photonics Research (IPR) Topical Meetings. He served as the Chair of the IPR sub-committee IV, Nanostructure Photonics, in 2001.